



## Deliverable 1.2: Measured lattice parameters, including lattice strain as a function of Hex-SiGe composition.

**Task 1.2.** (JKU)“Measurements of the Hex- $\text{Si}_x\text{Ge}_{1-x}$  lattice parameters and strain distribution for  $0 \leq x \leq 1$ ”. The lattice parameters and strain state of ensembles of NWs will be measured by advanced X-ray diffraction techniques in the lab and at synchrotrons and will be used as input for the DFT band structure calculations.

**D1.2** Measured lattice parameters, including lattice strain as a function of Hex-SiGe composition. [M18]

### General Overview

Hexagonally grown core-shell-shell (GaP/Si/Si<sub>x</sub>Ge<sub>1-x</sub>) nanowire-assemblies have been investigated using X-ray diffraction (XRD) in combination with numerical finite-element-model (FEM) simulations. The measurements in combination with the simulations were the basis to successfully establish methods to determine the relationship between the hexagonal Si<sub>x</sub>Ge<sub>1-x</sub> lattice parameters and the amount of Ge present. We could demonstrate the method on a systematic series of nanowire (NW) samples ranging from low (29%) up to comparatively high (77%) Ge concentration in the outer-most Si<sub>x</sub>Ge<sub>1-x</sub> shell (see Fig. 1). When performing comprehensive simulations on the mutual strain distribution coming from the core-shell-shell structure it turned out that the knowledge of the exact geometrical parameters (core diameter, shell thicknesses) of the wires has a crucial influence on the accuracy of the final results, the lattice parameter of the un-strained Hex-Si<sub>x</sub>Ge<sub>1-x</sub> material.

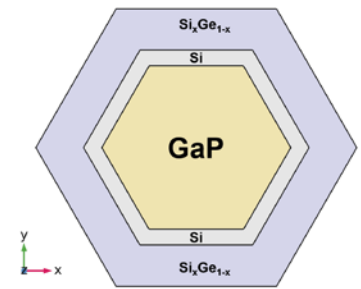


Figure 1 - Cross section of the NW. The inner most shell is hexagonal GaP followed by a thin Hex-Si shell and the outer most Hex-Si<sub>x</sub>Ge<sub>1-x</sub> shell.

### Samples

The investigated samples are core-shell-shell nanowires (NWs) which have in common a hexagonally grown GaP core followed by a first shell of Hex-Si. The outer most shell is an alloy of Hex-Si<sub>x</sub>Ge<sub>1-x</sub>. The cross-section of one wire is schematically depicted in Fig 1. In total 4 different samples with different Ge contents and different shell thicknesses have been successfully measured and simulated. The shell thicknesses as well as the exact composition (Si<sub>x</sub>Ge<sub>1-x</sub> shell) for each sample are provided by the TU Eindhoven and are measured by transmission electron microscopy (TEM) in combination with energy-dispersive X-ray spectroscopy (EDX), from a set of individual wires out of the ensemble. Detailed sample information on all measured and simulated samples is listed in the Tab.1.

Sample:	Ge %	SiGe Shell-thickness [nm]	Si Shell-thickness [nm]	GaP Core-radius [nm]
h03774	29.4	30.3	11.6	69
h03775	45.6	31.2	8	72
h03776	51.2	34.5	16	59
h03682	77	12	14	59

Table 1 - List of investigated samples

### X-ray diffraction measurements

X-ray diffraction measurements, for all listed samples have been performed at the *Deutsches Elektronen Synchrotron* (DESY) in Hamburg, at the high-resolution diffraction beamline P08. The diffraction experiments allow to directly access the different crystalline phases (cubic and wurtzite) and hence different lattice parameters (materials) present in the NW assemblies.

Each crystalline phase and each material (wurtzite or cubic / GaP, Si, Si-Ge) can be directly accessed via specific Bragg reflections. The measured NWs are composed out of three different materials (GaP, Si, and the  $\text{Si}_x\text{Ge}_{1-x}$  alloy) which induces a certain strain on-to each other due to the different native (un-strained) lattice constants (in- and out-of-plane). This leads to a complex strain distribution across the NW. When the materials are grown on top of each other they tend to mimic the in-plane lattice parameter of the material below, but can expand or compress in the direction perpendicular to the growth direction. One results of the inhomogeneous strain-field across the NW is that the measured Bragg reflection from each part (core-shell-shell) of the NW are smeared out and overlap in reciprocal space. Therefore, an easy separation of the different Bragg peaks stemming from the different core/shell materials of the NW is not possible. Rather, each single-measured NW Bragg reflection contains the information of all hexagonal core-shell-materials convolved with the complex strain distribution across the NW.

From each sample at least 2 reflection have been measured and simulated. Each measurement routine started with the hexagonal symmetric (000.6) reflection including the (333) GaP substrate reflection, which is the cubic equivalent and located next to the (000.6) reflection in reciprocal space coordinates. The second measured reflection is the hexagonal asymmetric (10-1.8) reflection. Fig. 2 indicates the different crystalline direction with respect to the geometry of the NW, directions marked in red correspond to directions in-line with measured Bragg reflections. The symmetric reflections are needed to determine, and hence to correct for any sample tilts and alignment offsets and because the intense GaP-substrate reflection in the symmetric reciprocal space maps is clearly visible and can be used as an “anchor” point. The position of the substrate reflection in reciprocal space is well defined due to the high crystalline quality of the substrate material and can be used as a reference. Reciprocal space maps around a symmetric and an asymmetric Bragg reflection for sample *h03774*, 29% Ge, can be seen in Fig. 3.

The positions, sizes and shapes of the measured Bragg peaks (in Fig. 3) are on the one hand defined by the different materials (GaP-Si-  $\text{Si}_x\text{Ge}_{1-x}$ ) and on the other hand also result from the mutual strain distributions affecting the core as well as the shell materials. The reciprocal space maps, as measured (and shown), are used as a basis for the final simulation routine that reconstructs the size and shape of the Bragg reflections using the strained core-shell-shell materials as input parameters.

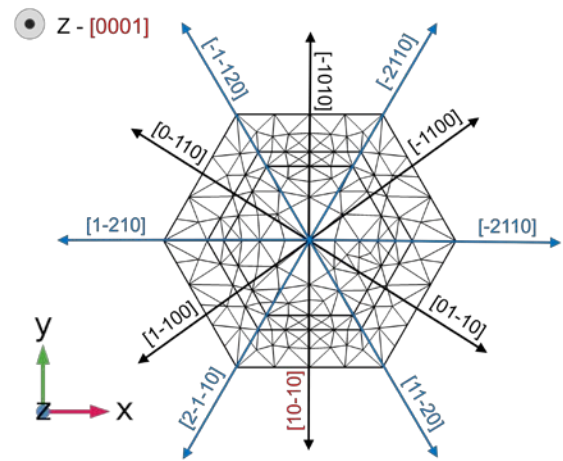


Figure 2 - Cross section of the NW, the red and blue arrows indicating the crystalline directions in Miller-Bravais notation. Each set of red/blue arrows corresponds to indistinguishable crystalline directions. The crystal planes marked in red are the equivalents to the measured reflections.

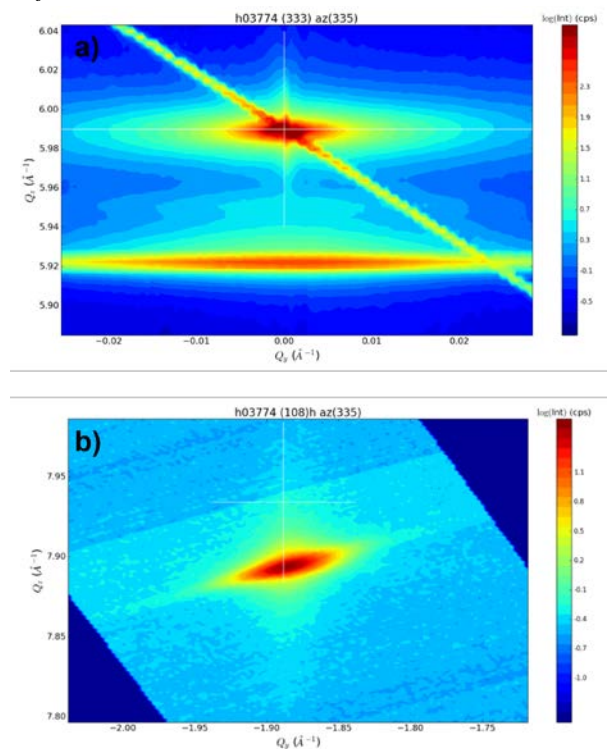


Figure 3a shows the measured reciprocal space map around the (000.6) Bragg reflection. The bright spot that appears at higher  $Q_z$  values is the GaP substrate and the area with the broad intensity distribution, that can be seen at lower  $Q_z$  values (higher out of plane lattice parameter), comes from the NWs. In b) a reciprocal space map around the (10-1.8) reflection is shown, this specific reflection is only allowed for nanowires, hence no substrate reflection can be measured at this position in reciprocal space.

## Simulations

The simulation routines are needed to identify the fraction of each different material contributing to the measured diffraction patterns (Bragg peaks) and to consequently “decompose” the diffraction patterns to extract the information about the native Si-Ge lattice constants. Basis for the simulation routines are a FORTRAN XRD code-package written by Václav Holý (Charles University, Prague) that allows to simulate diffraction patterns for a given set of materials. This code-package is used in combination with the commercially available FEM software COMSOL. The FEM software is used to create a wire-model to calculate the mutual strain-distribution within the different core-shell-shell wire-materials, assuming a pseudomorphic, defect free growth of each material on-top of each other.

In the first step a model of the NW is created, based on the geometry parameters (length and thicknesses, core diameters) obtained by TEM/EDX at TU Eindhoven. The general geometry, shown in a wire-frame model that is used for the simulations, is depicted in Fig. 4.

In the second step the different materials for the model are defined, using already known hexagonal lattice parameters for the GaP-core (Kriegner 2013<sup>9</sup>) and the Si-shell (Hauge 2015<sup>8</sup>). The corresponding elastic constants for WZ-GaP, Hex-Si and Hex-SiGe are calculated from the elastic constants of the cubic polytypes according to (Martin 1972<sup>1</sup>). For Hex-SiGe, the elastic constants ( $C_{ij}$ ) are linearly interpolated between Si and Ge, according to the Ge content ( $X_{Ge}$ ), determined by EDX at TU Eindhoven:

$$C_{ij-SiGe-WZ} = (1 - X_{Ge}) * C_{ij-Si-WZ} + X_{Ge} * C_{ij-Ge-WZ}$$

The lattice parameters  $\mathbf{a}$  (in-plane) and  $\mathbf{c}$  (out-of-plane) for the Hex-Si<sub>x</sub>Ge<sub>1-x</sub> shell are used as variable in-input parameters to create and compute, for each combination of  $\mathbf{a}$  and  $\mathbf{c}$ , an individual FEM model of the wire. The FEM model also takes into account the wire geometry (core-shell-shell thickness ratios have a high influence on the strain distribution across the wire) as a fixed in-put.

Along the growth direction, or  $\mathbf{c}$ -direction, the strain within each shell is observed to be homogenous except for the edge regions where the wire is “clamped” to the substrate, or at the top-region where the wire can freely relax. The in-plane strain distribution is observed to strongly vary across the wire cross-section and is a consequence of compressive or tensile lattice deformations due to pseudomorphic growth. Figure 5 a) and b) shows the spatial variation of the radial and tangential strain components across the NW for two different Ge contents in the Si<sub>x</sub>Ge<sub>1-x</sub> shell.

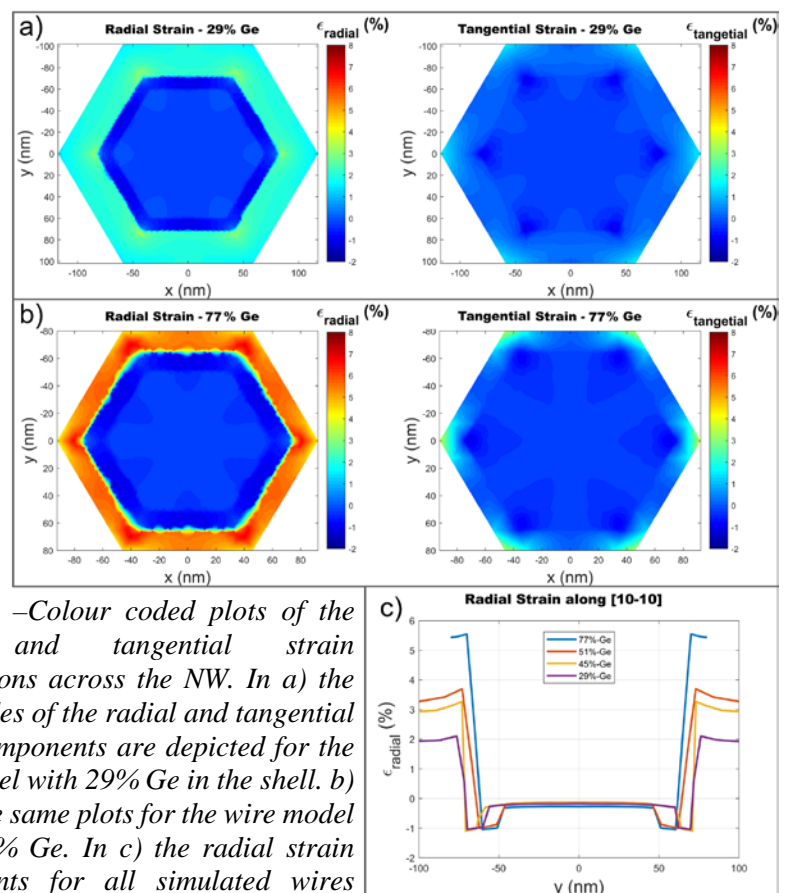


Figure 5 –Colour coded plots of the radial and tangential strain distributions across the NW. In a) the magnitudes of the radial and tangential strain components are depicted for the wire model with 29% Ge in the shell. b) shows the same plots for the wire model with 77 % Ge. In c) the radial strain components for all simulated wires (77%-51%-45% and 29% Ge in the outer-most shell) along the [10-10] direction are plotted.

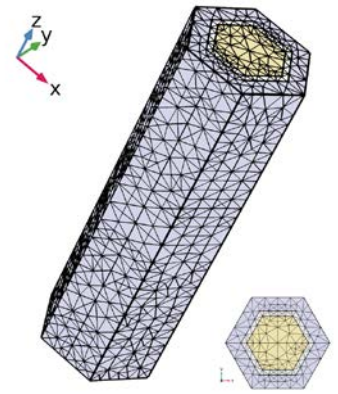


Figure 4 – Wire-frame model of one individual NW, as simulated. The different materials are colour-coded, identical to Fig. 1. The upper picture shows the full wire and the picture on the bottom shows the wire cross-section.

<sup>1</sup> Martin, Richard M. (1972): Relation between Elastic Tensors of Wurtzite and Zinc-Blende Structure Materials. In *Phys. Rev. B* 6 (12), pp. 4546–4553.

<sup>8</sup>H. I. T. Hauge, *Nano letters* 15 (2015) 5855

<sup>9</sup>D. Kriegner, *Phys. Rev. B* 88 (2013) 1559.

For a comparatively large SiGe shell (30nm) and a low Ge content (29%), as depicted in Fig. 5 a), the average radial strain in the outer SiGe-shell is around 2%, the inner Si-shell is compressively strain by about -1% and the GaP core is nearly unstrained. For the combination of a thin SiGe shell (12nm) and a high Ge content (77%) as depicted in Fig. 5 b) the average radial strain reaches values around 5%, the GaP-core and Si-shell have radial strain values comparable to the sample with 29% Ge. In Fig. 5 c) the radial strain distribution along the [10-10] in-plane crystalline direction (see Fig. 2) is plotted, the core and the Si-shell show similar radial-strain values, independent of the Ge-content, whereas the strain induced in the outer most SiGe shell is highly affected by the Ge content (as expected) and the shell thickness. The higher the Ge-content the higher is also the observed strain. The simulations in general show that the GaP core is nearly unstrained whereas the inner Si-shell shows compressive in-plane (radial) strain and the Si-Ge shell shows tensile in-plane (radial) strain. The GaP core is mostly un-affected by the lattice parameter mismatch to the Si-shell because much more GaP material is present, compared to the thin Si-shells. On the other hand, the inner Si shell is highly affected by the GaP core and the Si-Ge alloy, both having a higher in- and out-of-plane lattice parameter than native Hex-Si.

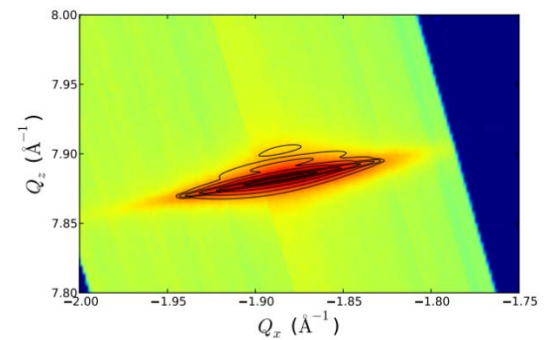


Figure 6 – Measured and simulated [1-108] Bragg peaks are plotted on-top of each other. The simulated Bragg peak, indicated by the black contour lines exactly reproduces the measurements for a certain combination of lattice parameter  $a$  and  $c$ .

The FEM simulations on the strain distributions performed with COMSOL are used as an input to calculate the corresponding diffraction patterns. These simulated patterns are then subsequently compared to the measured Bragg reflection. The native in- and out-of-plane  $\text{Si}_x\text{Ge}_{1-x}$  lattice parameters are varied until the simulated diffraction pattern coincides with the measured one. This procedure finally allows to determine the native lattices parameters of unstrained, Hex-  $\text{Si}_x\text{Ge}_{1-x}$ . In Fig. 6 a direct comparison between the simulated (10-18) Bragg peak (indicated by black contour-lines) and the measured (10-18) Bragg peak is shown. The simulation and the measurements perfectly match each other.

The simulations sensitively depend on the accurate knowledge of the shell-thicknesses as well as on the Ge contents which both highly influences the strain distribution.

## Results

A full samples series with different Ge contents, ranging from 29% up to 77 % Ge, has been successfully characterized. For all mentioned samples the native/un-strained in- and out-of-plane lattice parameters (**a** and **c**) of the Hex-Si<sub>x</sub>Ge<sub>1-x</sub> shell could be calculated combining XRD measurements and FEM simulations. The results are shown in Tab. 2 and Fig 6. In Fig 6. the lattice parameters (**a**, **c**) are plotted as a function of the Ge-content. Tab. 2 shows the exact values of the individual data-points obtained for each sample. When looking at the linear interpolation (blue dashed line in Fig.6) all measured data points show a rather weak scattering, indicating a high data-quality and low error bars. Nevertheless, the error-bars shown in Fig 6 have been estimated rather conservatively ( $\pm 0.2\%$  of the calculated data point), in terms of taking into account all geometrical and compositional uncertainties due to statistical deviations from wire to wire, that can't be avoided.

Sample:	Ge %	Lattice param. - a [ $\text{\AA}$ ]	Lattice param. - c [ $\text{\AA}$ ]
<i>h03774</i>	29.4	3.9084	6.4095
<i>h03775</i>	45.6	3.9234	6.4402
<i>h03776</i>	51.2	3.9504	6.4495
<i>h03682</i>	77	3.9984	6.5325

Table 2 - Calculated lattice parameters

Performing a linear interpolation through all calculated data points and the known data for Hex-Si (literature value), a linear relationship between the lattice contents as a function of the Ge constant can be established. This allows to provide an accurate estimation for the hexagonal lattice parameter for an arbitrary Hex-Si<sub>x</sub>Ge<sub>1-x</sub> alloy, with Ge contents ranging from 0%, pure Hex-Si, up to 100% Hex-Ge without the need of characterizing each sample individually any more. The corresponding equations can be written as:

$$\text{Linear interpolation, lattice parameter } a \rightarrow a = \text{Ge}_{\text{content}}(\%) * 0.00234 + 3.82421$$

$$\text{Linear interpolation, lattice parameter } c \rightarrow c = \text{Ge}_{\text{content}}(\%) * 0.00264 + 6.3237$$

Furthermore, the knowledge of the lattice parameters allows to do strain calculations on certain Ge-concentrations and shell-thicknesses in-advance which can then be used for an intentional manipulation of the band-structure via strain as tuning knob.

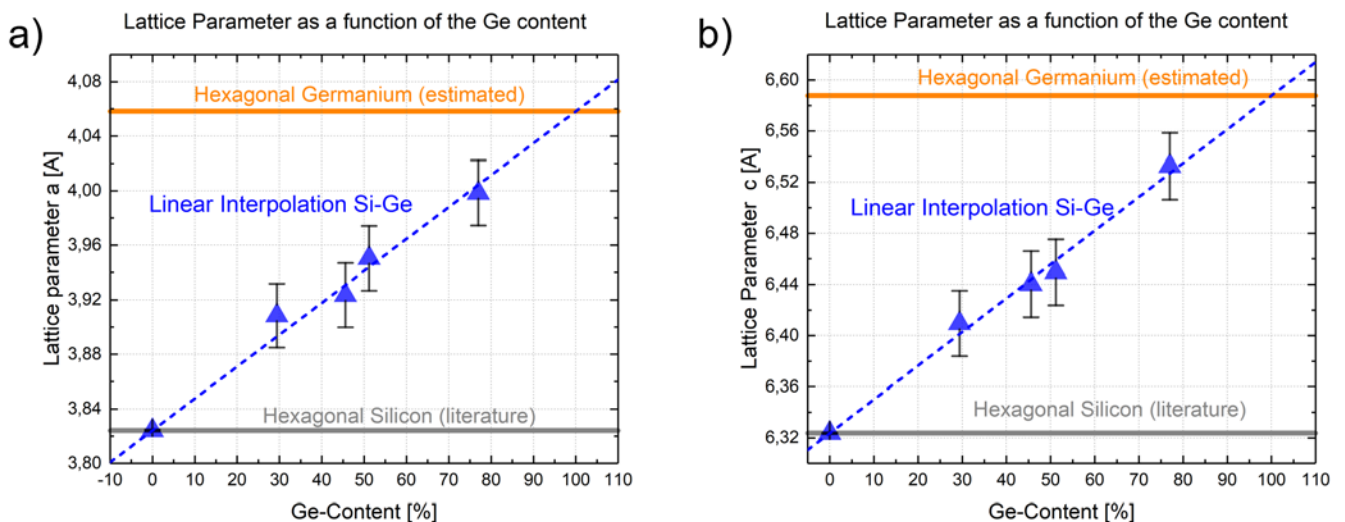


Figure 7 - a) shows the lattice parameter *a* of Hex-Si<sub>x</sub>Ge<sub>1-x</sub> as a function of the Ge content for all measured samples. The orange line indicates the estimated native lattice parameter of pure Hex-Ge and the grey line the, by literature, known lattice parameter of Hex-Si. In b) the lattice parameter *c* is shown as a function of the germanium content. The blue dashed lines show a linear interpolation through all datapoints.